La granja:
Revista de
Ciencias de la Vida
pISSN:1390-3799; eISSN:1390-8596
http://doi.org/10.17163/lgr.n34.2021.02

Special Issue / Edición Especial
Geospatial Science

Spectral characterization and monitoring of mangrove forests with remote sensing in the Colombian Pacific Coast: Bajo Baudó, Chocó

Caracterización espectral y monitoreo de bosques de manglar con Teledetección en el litoral Pacífico colombiano: Bajo Baudó, Chocó

Mauricio Alejandro Perea-Ardila*[1], Julian Leal-Villamil[2] and Fernando Oviedo-Barrero[1]

[1] *Pacific Oceanographic and Hydrographic Research Center-CCCP, Integrated Coastal Zone Management Area, Port Captaincy of Tumaco. Tumaco, Colombia.*
[2] *Interdisciplinary Research Group in Tropical Fruit Growing. University of Tolima, Santa Helena neighborhood high part, Ibagué, Colombia.*

*Corresponding author: mapereaa@ut.edu.co

Article received on February 25th, 2021. Accepted, after review, on May 25th 2021. Published on September 1st, 2021.

Abstract

The Colombian Pacific has extensive areas in mangrove forests (MF), which is a strategic ecosystem of great environmental and socioeconomic for climate change mitigation. This work aimed to perform spectral characterization and monitoring of 66.59 km2 for four MF densities in Bajo Baudó (Colombia), using three Landsat images (1998, 2014 and 2017), combinations of spectral bands and three vegetation indices (VI) (Normalized Difference Vegetation Index-NDVI, Soil Adjusted Vegetation Index-SAVI and the Combined Mangrove Recognition Index-CMRI). The results showed that the best combination of spectral bands for visual identification of MF corresponded to infrared color (NIR, Red, Green) and false-color composite 1 (NIR, SWIR, Red). The spectral sign of MFs had different behaviors in four densities under the conditions of high tide and low tide. During the 19 years analyzed, there was a difference of up to 17.9% in the average reflectance value in MF. Similarly, the values of VI were proportional to the densities of MF, but their value was reduced by tidal effects at the time of capturing the images; the largest increases in VI were recorded over the coastal area of land-water transition, where there is a strong interaction with the tidal condition. This research contributes to the spatial characterization and monitoring of MF with remote sensors and the spectral study of this important ecosystem in Colombia.

Keywords: Tide, spectral signature, vegetation indexes, Landsat, reflectance.

Resumen

El Pacífico colombiano posee extensas zonas en bosques de manglar (BM), que es un ecosistema estratégico de gran importancia ambiental y socioeconómica para la mitigación del cambio climático. Este trabajo tuvo por objetivo realizar la caracterización espectral y monitoreo de 66,59 km2 para cuatro densidades de BM en el Bajo Baudó (Colombia), empleando tres imágenes Landsat (1998, 2014 y 2017), combinaciones de bandas espectrales y tres índices de vegetación (IV) (Índice de Vegetación de Diferencia Normalizada-NDVI, Índice de Vegetación Ajustado al Suelo-SAVI y el Índice combinado de reconocimiento de manglares-CMRI). Los resultados demostraron que la mejor combinación de bandas espectrales para la identificación visual de los BM correspondió a infrarrojo color (NIR, Rojo, Verde) y falso color compuesto 1 (NIR, SWIR, Rojo). La firma espectral de los BM tuvo diferentes comportamientos para las cuatro densidades bajo las condiciones de pleamar y bajamar. Durante los 19 años analizados, se registró una diferencia de hasta el 17,9 % en el valor promedio de la reflectancia en los BM. De igual manera, los valores de IV fueron proporcionales a las densidades de BM, pero su valor se notó reducido por efectos de la marea al momento de la captura de las imágenes; los mayores aumentos de IV se registraron sobre la zona costera de transición tierra-agua donde existe una fuerte interacción con la condición mareal. Esta investigación aporta a la caracterización y monitoreo espacial de BM con sensores remotos y el estudio espectral de este importante ecosistema en Colombia.

Palabras clave: Marea, firma espectral, índices de vegetación, Landsat, reflectancia.

Suggested citation: Perea-Ardila, M., Leal-Villamil, J. and Oviedo-Barrero, F. (2021). Spectral characterization and monitoring of mangrove forests with remote sensing in the Colombian Pacific Coast: Bajo Baudó, Chocó. La Granja: Revista de Ciencias de la Vida. Vol. 34(2):26-42. http://doi.org/10.17163/lgr.n34.2021.02.

Orcid IDs:

Mauricio Alejandro Perea-Ardila: http://orcid.org/0000-0003-4561-0251
Julian Leal-Villamil: http://orcid.org/0000-0002-5100-2693
Fernando Oviedo-Barrero: http://orcid.org/0000-0001-5559-1504

1 Introduction

Mangrove forests (MF) are ecosystems that are very important for coastal zones of tropical and subtropical countries; they are relevant for the preservation as they host a large number of species of flora and fauna, and are vital and represent an economic source for rural communities (FAO, 2007; Monirul et al., 2018). Mangroves are key to the carbon cycle and climate change mitigation actions (Kuenzer et al., 2011; Giri, 2016; Pham et al., 2019). Despite the multiple benefits, worldwide MF are strongly degraded, mainly due to agricultural activities, urban expansion, coastal development and induced phenomena such as sea-level rise (Rhyma et al., 2020); therefore, regular monitoring in the MF is necessary to contribute to the ecosystem and to serve as a planning tool for the preservation of ecosystem services for future generations (FAO, 2007).

MFs are located in intertidal areas that are difficult to access and with varying environmental conditions that largely limit logistical aspects to conduct periodic monitoring in the field (Zhang et al., 2017; Jia et al., 2019). In this regard, Remote Sensing is a valuable tool for monitoring these ecosystems, as it allows monitoring of the MF at regional and local scales (Giri, 2016; Muhsoni et al., 2018). MFs are easily identifiable in the infrared bands due to the amount of moisture in the vegetation (Purwanto and Asriningrum, 2019). These spectral characteristics also determine the measurement of photosynthetic activity of the MF by using vegetation indices (IV) (Bannari et al., 1995; Rhyma et al., 2020).

The Normalized Difference Vegetation Index (NDVI) proposed by Rouse et al. (1974) is one of the most used for the study of vegetation worldwide (Chuvieco, 2010); this IV has as its main characteristic in the relationship between infrared and red bands, which efficiently determines the differences in the absorption of light from plants (Asner, 1998). NDVI has been widely used for monitoring MF and has an easy interpretation since it has a measuring range of -1 to +1, where positive values reflect areas with vegetation (Rhyma et al., 2020).

On the other hand, The Soil-Adjusted Vegetation Index (SAVI) (Huete, 1988) was developed to eliminate the influence of soil on reflectance absorption by vegetation, this includes the L parameter which can obtain values between 0 and 1 to eliminate the effect of the soil, i.e., is an improved NDVI (Bannari et al., 1995). The Combined Mangrove Recognition Index (CMRI) was developed by Gupta et al. (2018) to uniquely identify MF; its main characteristic is the subtraction between the NDVI and the NNormalized Difference Water Index (NDWI), facilitating the recognition of the BM since it incorporates the moisture content of the vegetation. The CMRI has a measurement range between -2 and +2, where positive values represent areas with MF. The use of spectral parameters and the specific development of IVs has allowed great advances in obtaining the quantitative and qualitative information necessary for the characterization of MF in different zones (Conti et al., 2016).

Different studies worldwide have incorporated the use of remote sensor images and remote sensing techniques for mangrove monitoring; this is the case with Rebelo-Mochel and Ponzoni (2007), who used Landsat 5 TM images and field data to characterize four species in MF in Turiau Bay, northeastern Brazil. Omar et al. (2018) used Landsat images for spectral signature characterization and implemented the use of IV to monitor changes in Malaysia's MF for three dates (1990, 2000 and 2017). Similarly, Ávila et al. (2020) determined the spatial-temporal variation of MF in Cuba using Landsat data for 35 years (1984 - 2019) and implemented two IVs (NDVI and EVI) in their monitoring for conservation purposes. Umroh and Sari (2016) used false color combinations in Landsat and NDVI images to monitor the different densities of MF on Pongok Island in Indonesia. Additionally, Rhyma et al. (2020) used NDVI and different L parameter setting values in the SAVI index for MF monitoring, using medium spatial resolution images at the Matang reserve in Malaysia. For his part, Chen (2020) implemented the use of CMRI and NDVI for monitoring MF in Dongzhaigang (China) with medium-resolution satellite images.

At the regional level, Galeano et al. (2017) used images from high-resolution remote sensors incorporating NDVI and climate factors in MF monitoring in the Rosario Islands in the Colombian Caribbean. Perea-Ardila et al. (2019) mapped dense MF in the municipality of Buenaventura, central zone of the Colombian Pacific, and detailed some basic spectral signatures of this ecosystem using Sentinel

2 images. The studies mentioned above highlight the importance of the use of remote sensing for the characterization of MF, monitoring at different scales and with different methodological approaches.

Colombia, along the Pacific coast, has approximately 2094,03 km^2 mangrove forests (Rodríguez-Rodríguez et al., 2016), an area that can correspond to 70 and 80% of the country's total MF (Wilkie and Fortuna, 2003). This ecosystem requires constant monitoring, as it provides multiple ecosystem services in terms of conservation and is considered to be an ecosystem highly threatened by climate change (Chow, 2017). The aim of this paper is to use remote sensing techniques and three vegetation indices (NDVI, SAVI, CMRI) to characterize spectrally and monitor four densities of MF using three-year Landsat images (1998, 2014 and 2017) in different tidal states in Lower Baudó – Chocoano. With the results obtained in this research, progress will be made in the spectral study and spatial monitoring of MF with Landsat images in strategic coastal ecosystems of Colombia.

2 Materials and methods

2.1 Study area

The study area was located in the north of the Colombian Pacific, on the coastal area of the municipality of Bajo Baudó, Chocó (Figure 1). According to the classification of life zones established by Holdridge (1978), the area corresponds to a Tropical Very Humid Forest (bmhT). Annual precipitation ranges from 4000 to 7000 mm of rain and has an average annual temperature of more than 24°C (Blanco et al., 2014). Land geoforms and climatic conditions in the area lead MF to be mostly on the coast, with heights above 40 m (Rodríguez-Rodríguez et al., 2016).

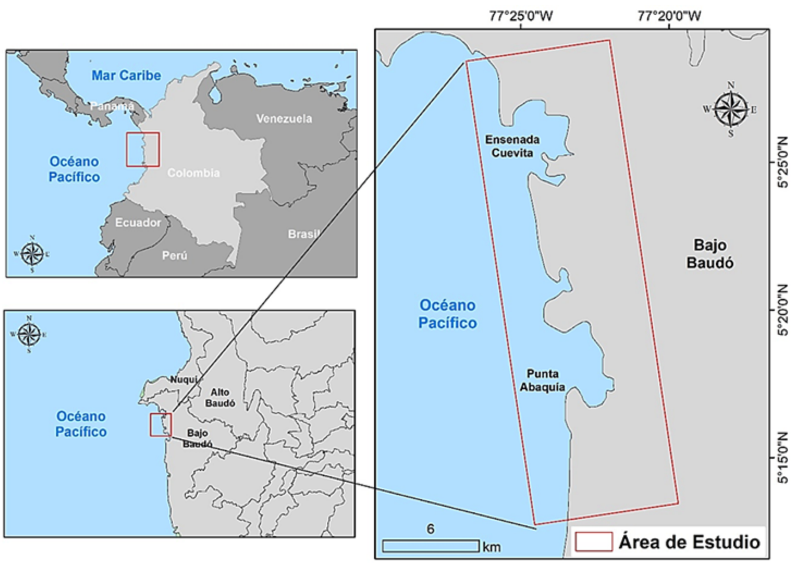

Figure 1. Location of the study area.

The flow diagram used in this research is presented in Figure 2. It was observed in the processes used (i) the digital processing of Landsat images, (ii) spectral signature analysis of mangrove forests by spectral sign and (iii) calculation of vegetation indices for different mangrove densities. Similarly, geospatial data management and analysis of Landsat images was performed using ArcGIS 10.3 software (ESRI, 2014).

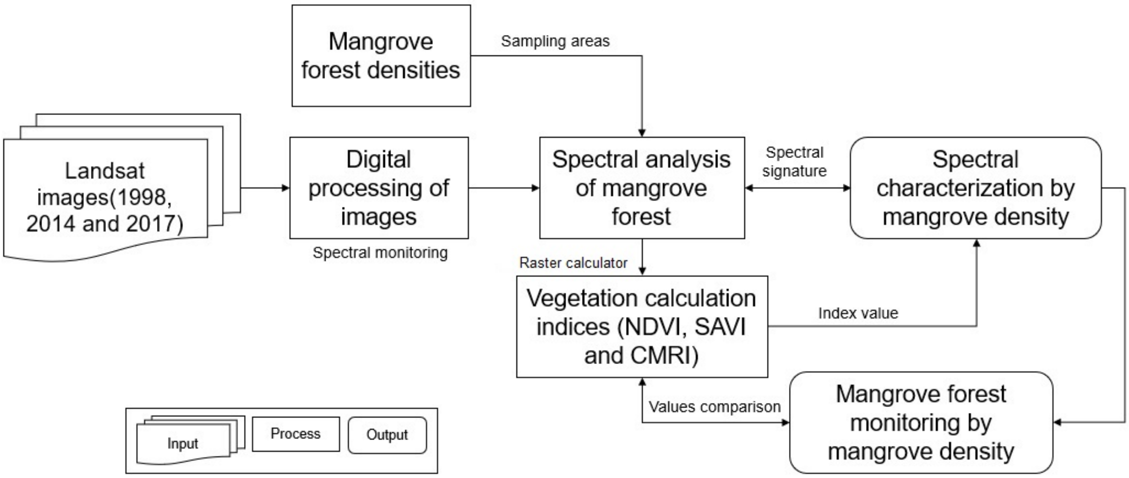

Figure 2. Flow diagram used.

2.2 Remote sensor images

Three Landsat images with 30 m spatial resolution for the years 1998, 2014 and 2017 ((USGS, 1998, 2014, 2017) were freely downloaded through the official website of the U.S. Geological Survey (USGS) https://earthexplorer.usgs.gov/ (USGS, 2020). The selection of the images corresponded to products that did not present cloud affectation, since this area presents high cloudiness during most of the year (Table 1).

Information on marine conditions was identified on the basis of data from the RedMPOMM (Ocean Parameters and Marine Meteorology Monitoring Network) of Colombia, of the Maritime General Office (https://geohub-dimar.opendata.arcgis.com/) (Dirección General Marítima., 2020). In this step, the date and time of the Landsat image was identified and validated with respect to the tide conditions recorded for that time.

2.3 Pre-processing of satellite images

Images underwent pre-processing; their digital levels (DL) were transformed to physical units (full-time reflectance at the Top of Atmosphere-ToA) using the parameters for reflectance normalization established by Ariza (2013); USGS (2018b) for Landsat 8 and Chander and Markham (2003); USGS (2018a) for Landsat 5 and 7, respectively (Table 2). Similarly, the images were cut out according to the study area, then the band fusion was carried out for their respective analysis.

2.4 Definition of mangrove forest densities

Vectorized 2019 data for the 1:2000 scale MF density developed by the Pacific Oceanographic and Hydrographic Research Center (CCCP) (DIMAR-CCCP, 2013) were used. This mapping was performed under visual image interpretation techniques using very high spatial resolution orthophotos and Light Detection and Ranging (LIDAR), which have the spatial characterization of the different MF in relation to their density and height, allowing to establish four density categories corresponding to: High Dense Mangroves (MDA), High Open Mangrove (MAA), Low Dense Mangrove (MDB) and Low Open Mangrove (MAB). A mask was made with this layer, where the limits of mangrove coverage were defined in Landsat images and their corresponding densities were determined.

2.5 Spectral analysis of mangrove forests

To observe the behavior of MF at different wavelengths, 4 combinations of bands described by Horning (2014); Franco (2017) were used, which were: True color (Red, Green, Blue), Infrared color (NIR, Red, Green) and composite false color 1 (NIR, SWIR, Red) and composite false color 2 (SWIR, NIR,

Table 1. Characteristics of the Landsat images used.

Characteristics	Landsat 5 TM	Landsat 8 OLI	Landsat 7 ETM+
ID Product	LT50100561998003CPE00	LC80100562014239LGN01	LE70100562017111EDC00
Capture date	03/01/98	27/08/14	21/05/17
Column/Row		010 - 056	
Cloud cover	16.00 %	18.53 %	21.00 %
Solar angle	46.62°	63.51°	64.39°
Fubmetric resolution	8 Bits	12 Bits	8 Bits
	Band 1 - Blue (0.45-0.52)	Band 2 - Blue (0.45-0.51)	Band 1 - Blue (0.45-0.52)
	Band 2 - Green (0.52-0.60)	Band 3 - Green (0.53-0.59)	Band 2 - Green (0.52-0.60)
Wavelength	Band 3 - Red (0.63-0.69)	Band 4 - Red (0.64-0.67)	Band 3 - Roja (0.63-0.69)
	Band 4 - NIR (0.77-0.90)	Band 5 - NIR (0.85-0.88)	Band 4 - NIR (0.77-0.90)
	Band 5 - SWIR1 (1.55-1.75)	Band 6 - SWIR1 (1.57-1.65)	Band 5 - SWIR1 (1.55-1.75)
Tide state	Unknown	High tide	Low tide
Projection		UTM zone 18	

Based on the metadata of the images and tidal records of the RedMPOMM.

Red). Polygons for cloud masking were digitized for each image to avoid the influence of clouds and shadows in spectral analysis of MF (Zhu and Woodcock, 2014; Pimple et al., 2018). In accordance with Congalton's statistical sampling recommendations for spectral analysis (Congalton, 1991), a random set of 200 sampling points distributed equally among the different MF densities (50 for each established density) was established, the average ToA reflectance values were established for each image, and the corresponding spectral signs were recorded in the evaluated time period.

2.6 Calculation of Vegetation Indices

To monitor MFs in the selected time period, the IV indices described in Table 3 were used.

2.7 Mangrove forest monitoring with vegetation indices

A comparison was made between IV values, taking into account MF densities for 1998-2014, 2014-2017 and 1998-2017 as a reference and identifying the variation in the IV value for each density. Graphical comparisons were made between the IV value and the MF density, where the behavior was determined for each period of time studied.

3 Results

3.1 Pre-processing of satellite images

NDs of the images were transformed to ToA reflectance values (Table 4), this process allowed to obtain a radiometric improvement by largely eliminating the atmospheric effects present in the original products. Images were also clipped to the study area and the clouds present in the study area were masked.

3.2 Mangrove forest density

According to the digital information described in DIMAR-CCCP (2013), the analysis of spatial distribution and MF density was carried out in the area of study; a total extension of MF was found of 66.59 km^2. The density of High Dense Mangrove (MDA) was the most predominant in the area, while Low Open Mangrove (MAB) presented the least extent in the study site (Table 5).

Table 2. Calibration Parameters of Landsat 8 images.

Sensor	Equation
Landsat 5 TM Landsat 7 ETM+	$L_\lambda = \left(\frac{LMAX_\lambda - LMIN_\lambda}{Qcalmax - Qcalmin}\right)(Q_{cal} - Q_{calmin}) + LMIN_\lambda$ $\rho_\lambda = \frac{\pi L_\lambda d^2}{ESUN_\lambda cos\theta_s}$ With: L_λ: Spectral radiation at the sensor opening $[W/(m^2 sr \mu m)]$. $Qcal$: Calibrated pixel quantified value $[DN]$. $Qcalmin$: The minimum quantified value of the calibrated pixel $[DN]$. $Qcalmax$: The maximum quantified value of the calibrated pixel $[DN]$. $LMIN_\lambda$: Spectral radiance at the sensor that scales to Qcalmin $[W/(m^2 sr\ \mu m)]$. $LMAX_\lambda$: Spectral radiance on the sensor that scales to Qcalmax $[W/(m^2 sr\ \mu m)]$. ρ_λ: Planetary reflectance of the ToA. d: Earth-Sun distance [astronomical units]. $ESUN_\lambda$: Exoatmospheric mean solar irradiance $[W/(m^2)]$. θ_s: Solar zenithal angle.
Landsat 8 OLI	$\rho'_\lambda = \frac{M_p Q_{cal} + A_p}{sen\theta_{se}}$ With: ρ'_λ: Planetary reflectance or on top of the atmosphere-ToA. M_p: Specific scaling multiplicative factor. Q_{cal}: Calibrated pixel quantified value. A_p: Specific scaling additive factor. θ_{se}: Solar elevation angle of the center of the scene.

3.3 Spectral analysis of mangrove forests

Four spectral combinations were obtained for satellite products, and MF could be visually distinguished from other plant coverages (Table 6). The true color combination showed that the vegetation of MF showed dark green tones and a low brightness for the image of 1998 and 2014, and slightly lighter green tone for the image of 2014 that is not influenced by tide. For the infrared color combination, MF showed dark red tones and low brightness; the 2014 image in high tide showed a much lower brightness, highlighting the large moisture content of the vegetation compared to other plant coverings that presented reddish to pinkish tones. Similarly, for the composite false color 1 combination, MF showed a brown color with a dark tone for the image of 1998 and 2014, showing large moisture content in the vegetation and great contrast against other coverages. The composite false color combination 2 revealed a moderately dark green coloring, allowing easy recognition of coverage; however, differences in tones with respect to the tidal state were observed

Table 3. Description of the vegetation indices and water index used in this study.

Index	Equation	Reference
Normalized Difference Vegetation Index (NDVI)	$\frac{NIR - Red}{NIR + Red}$	Rouse et al. (1974)
Soil-Adjusted Vegetation Index (SAVI)	$\frac{NIR - Red}{NIR + Red + L}(1+L)$	Huete (1988)
Normalized Difference Water Index (NDWI)*	$\frac{Green - NIR}{Green + NIR}$	Gao (1996)
Combined Mangrove Recognition Index (CMRI)	NDVI-NDWI	Gupta et al. (2018)

With: L=0.5. *NDWI was only used to determine CMRI.

Table 4. Statistical summary of reflectance values obtained from Landsat images.

Parameters	Landsat image used														
	Landsat TM (1998)					Landsat OLI (2014)					Landsat ETM+ (2017)				
	B1	B2	B3	B4	B5	B2	B3	B4	B5	B6	B1	B2	B3	B4	B5
Min	0.00	0.00	0.00	0.01	0.00	0.07	0.04	0.02	0.00	0.00	0.01	0.01	0.01	0.03	0.00
Max	0.44	0.89	0.76	0.95	0.63	0.75	0.75	0.79	0.90	0.59	0.34	0.38	0.35	0.80	0.50
Av	0.03	0.05	0.03	0.17	0.07	0.10	0.08	0.06	0.20	0.09	0.03	0.04	0.03	0.32	0.13
Std	0.03	0.05	0.03	0.14	0.05	0.04	0.04	0.05	0.15	0.06	0.03	0.03	0.03	0.19	0.07

With B1 (Band 1), B2 (Band 2), B3 (Band 3), B4 (Band 4), B5 (Band 5), Minimum (Min), Maximum (Max), Average (Av) and Standard deviation (Std).

3.4 Mangrove forest spectral sign

The spectral sign for ToA reflectance was calculated for all three images (Figure 3). It was found that the average reflectance for NIR band of 2017 image with respect to the NIR reflectance of 2014 and 1998 showed a difference of 12.6% and 17.9%, respectively.

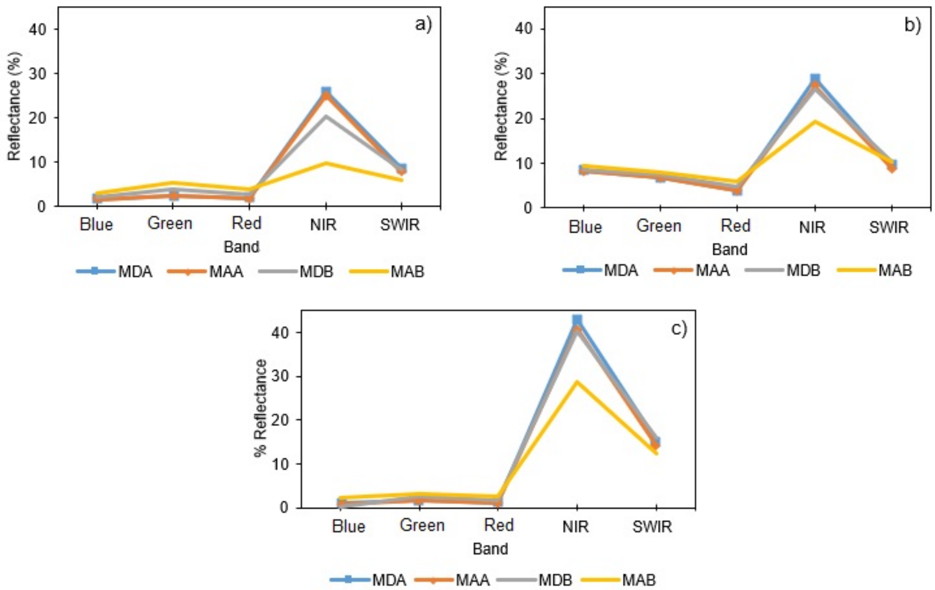

Figure 3. Spectral sign estimated for MF in Landsat products (a) 1998, (b) 2014 and (c) 2017. Where: High Dense Mangrove (MDA), High Open Mangrove (MAA), Low Dense Mangrove (MDB), Low Open Mangrove (MAB).

In all the cases presented, MF in their different densities (MDA, MAA, MDB, and MAB) showed higher reflectance values in the near infrared, being consistent with the average spectral sign of vegetation. In this sense, the minimum, maximum and average reflectance values recorded for each MF density are shown in Table 7.

3.5 Vegetation index

It was observed that values for MAB density in the three IVs in 1998 were the lowest with 0.28, 021 and 0.41 for NDVI, SAVI and CMRI, respectively (Figure 4). It was found that IV values tend to decrease slightly according to density, and it was also observed that high tide conditions in the 2014 image tend to have lower IV values than 2017 image. Ta-

Table 5. Density of mangrove forests present in the study area.

Mangrove density	**Description**	**Area (km^2)**	**Extension (%)**	**Detail**
High Density Mangrove (MDA)	Mangroves with heights above 15 m cwhose density represents more than 70 % coverage in their unit.	53.60	80.49	
High Open Mangrove (MAA)	Mangroves with heights above 15 m whose density represents between 30 and 70 % coverage in their unit.	9.8	13.94	
Low Density Mangrove (MDB)	Mangroves with heights lower than 15 m whose density represents more than 70 % coverage in their unit.	3.18	4.78	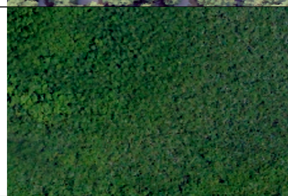
Low Open Mangrove (MAB)	Mangrove with heights below 15 m whose density represents between 30 and 70 % coverage in their unit.	0.53	0.8	
TOTAL		66.59	100.00 %	

ble 8 shows the minimum, maximum and average values of IVs recorded for each year at the different MF densities present in the study area.

3.6 Mangrove forest monitoring

An average increase in the value of NDVI and CMRI for MAB of 0.19 and 0.42 was observed between 1998-2014 (Figure 5). Increases were observed over coastal areas that are constantly interacting with the tide.

For its part, the period 2014-2017 recorded an increase for SAVI values of more than 0.5 in all densities. The period 1998-2017 recorded an average increase in NDVI and CMRI values of 0.09 and 0.35 for MDB and 0.31 and 0.95 for the MAB, respectively; Likewise, SAVI presented increases in value higher than 0.2 for all densities (Figure 6).

4 Discussion

The combination of spectral bands is a visual analysis technique that allows identifying different types of coverage through its spectral characteristics ((Chuvieco, 1995; Pérez and De la Riva, 1998; Horning, 2014; Mohamed, 2017). Its application to the MF is valid to the extent that combinations that highlight this coverage are used, such as the infra-

Table 6. Combinations of bands used in the research.

Combinations of bands			
True color	**Infrared color**	**False composite 1**	**False composite 2**
Landsat 5 - 1998			
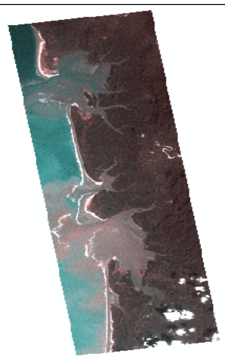	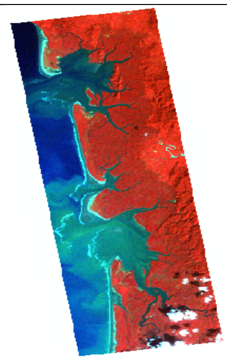	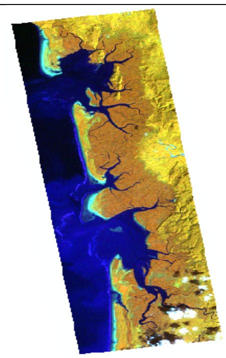	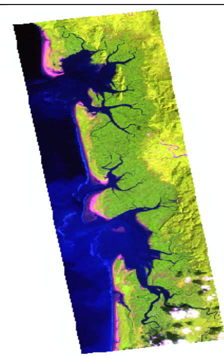
Landsat 8 - 2014			
	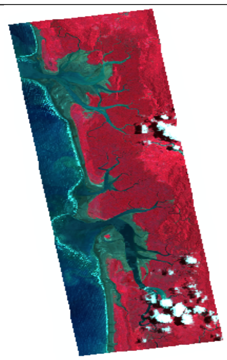	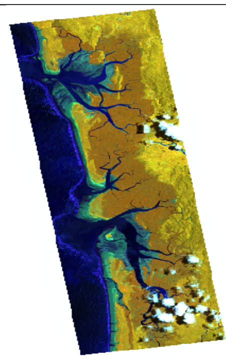	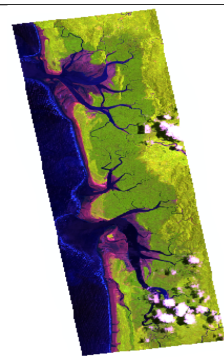
Landsat 7 - 2017			
	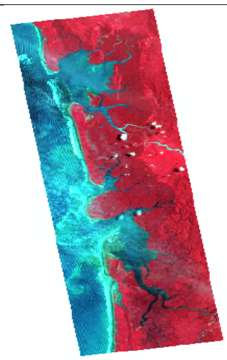	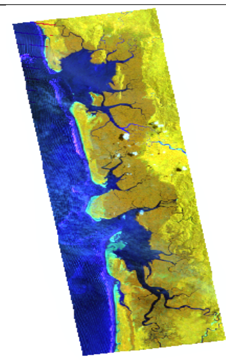	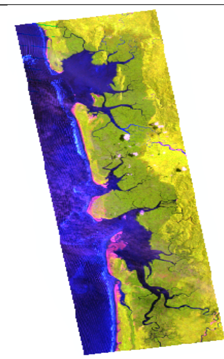

red color (NIR, Red, Green) and the false composite color 1 (NIR, SWIR, Red) in accordance with what is mentioned by Pagkalinawan (2014). However, an important aspect to consider when performing spectral analysis on MF is the presence of clouds and shadows, since this region has a large volume of precipitation (Blanco et al., 2014), which can greatly affect MF reflectance values and can be a limiting factor in performing multi-temporal analysis and primary changes as expressed by Pimple et al. (2018) and (Wang et al., 2019). While this study found low cloud coverage, masking removed a portion of the mangrove in the southern zone, causing uncertainty about the reflectance values for the removed area.

Table 7. Estimated average reflectance values for mangrove forest densities.

Band	Landsat 5 - 1998											
	MDA			MAA			MDB			MAB		
	Min	Max	Av	Min	Max	Av	Min	Max	Av	Min	Max	Av
Blue	0.8	2.8	1.5	0.8	2.5	1.5	1.2	4.3	2.1	1.0	6.7	3.0
Green	1.0	5.0	2.4	1.0	4.5	2.4	1.9	8.1	3.7	1.4	13.1	5.4
Red	0.9	2.9	1.8	0.9	2.6	1.7	0.9	6.3	2.7	1.6	8.3	3.8
NIR	16.5	32.8	26.0	13.3	30.5	25.0	2.1	31.0	20.3	1.6	32.8	9.8
SWIR	5.4	14.5	8.5	5.2	10.0	7.8	1.4	15.0	8.3	1.2	18.0	5.8
	Landsat 8 - 2014											
Blue	7.9	14.2	8.3	7.6	10.6	8.2	8.1	11.1	8.6	8.3	11.2	9.5
Green	6.2	12.8	7.0	5.4	9.1	6.8	6.1	9.6	7.5	6.8	9.8	8.1
Red	3.3	10.5	4.0	3.0	6.7	3.9	3.7	9.0	4.7	4.0	8.8	6.0
NIR	20.1	34.7	28.9	12.2	36.5	27.3	14.1	33.8	26.6	9.2	31.1	19.3
SWIR	7.1	15.7	9.6	3.8	11.3	8.9	5.7	13.0	10.4	7.0	16.2	10.4
	Landsat 7 - 2017											
Blue	0.3	2.7	1.0	0.0	2.3	0.7	1.2	3.2	0.3	0.5	4.7	2.2
Green	0.6	3.1	1.8	0.8	3.5	1.6	1.5	3.9	2.5	1.2	4.9	3.1
Red	0.5	2.4	1.2	0.5	2.8	1.0	0.9	3.4	1.8	1.1	4.7	2.7
NIR	28.2	51.2	43.0	1.8	48.9	40.8	16.1	48.9	40.2	12.0	47.2	28.7
SWIR	10.0	19.2	15.2	8.9	17.2	14.2	7.2	20.5	15.9	4.7	24.4	12.3

Where: Minimum (Min), Maximum (Max) and Average (Av).

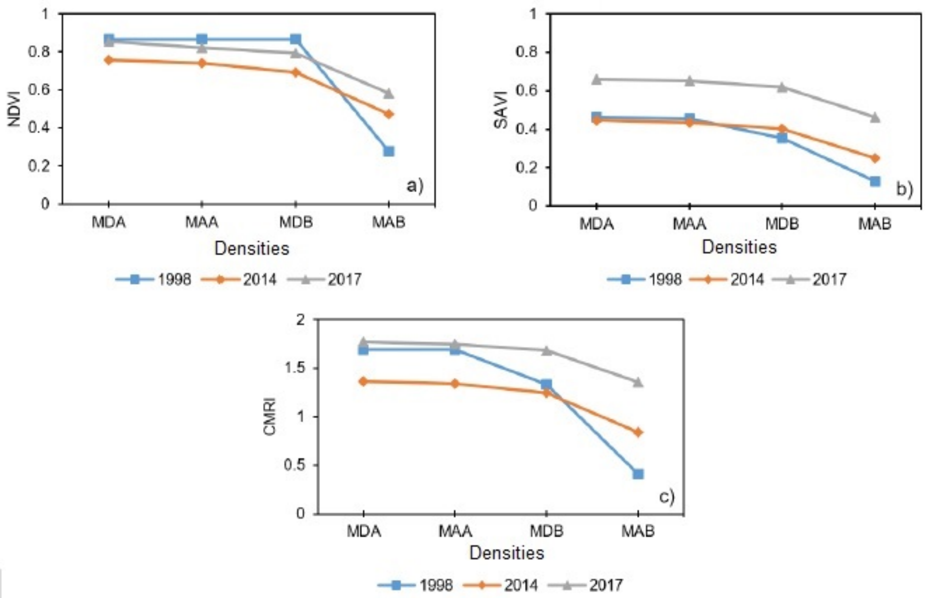

Figure 4. Estimated values for vegetation indices according to mangrove forest densities and analyzed season (a) NDVI (b) SAVI and (c) CMRI. Where: High Dense Mangrove (MDA), High Open Mangrove (MAA), Low Dense Mangrove (MDB), Low Open Mangrove (MAB).

The reflectance of the infrared band of 1998 and 2014 varied from that of 2017, between 12.6 and 17.9%, respectively; however, these values are within the range reported by authors such as Mondal et al. (2018) and Perea-Ardila et al. (2019). Moreover, MAB for 1998 had an average reflectance in the infrared band of 9%, which is close to that reported by Vaghela et al. (2018) for open mangroves in India. Low values in infrared reflectance can be caused by the high moisture content in mangroves by

Table 8. Values of vegetation indices for each mangroves density.

Index	Landsat 5 - 1998											
	MDA			**MAA**			**MDB**			**MAB**		
	Min	Max	Av	Min	Max	Av	Min	Max	Av	Min	Max	Av
NDVI	-0.6	0.96	0.87	-0.2	0.95	0.87	-0.6	0.96	0.87	-0.62	0.92	0.28
SAVI	-0.1	0.62	0.46	-0.03	0.58	0.45	-0.1	0.56	0.36	-0.1	0.62	0.13
CMRI	-1.3	1.93	1.69	-0.5	1.92	1.69	-0.9	1.86	1.34	-1.34	1.8	0.41
	Landsat 8 - 2014											
NDVI	-0.1	0.84	0.76	0.07	0.83	0.74	0.18	0.83	0.69	0.18	0.83	0.69
SAVI	0.03	0.63	0.45	0.02	0.58	0.43	0.07	0.62	0.4	12	0.57	0.25
CMRI	-0.4	1.56	1.37	-0.1	1.53	1.34	0.3	1.53	1.25	-0.01	1.5	0.84
	Landsat 7 - 2017											
NDVI	0.26	1.32	0.86	0.21	1.21	0.82	0.24	1.22	0.79	0.16	0.16	0.58
SAVI	0.29	0.83	0.66	0.15	0.79	0.65	0.26	0.78	0.62	115	0.74	0.46
CMRI	1.01	2.26	1.77	0.64	2.13	1.75	0.98	2.1	1.68	0.51	1.98	1.36

Where: Minimum (Min), Maximum (Max) and Average (Av).

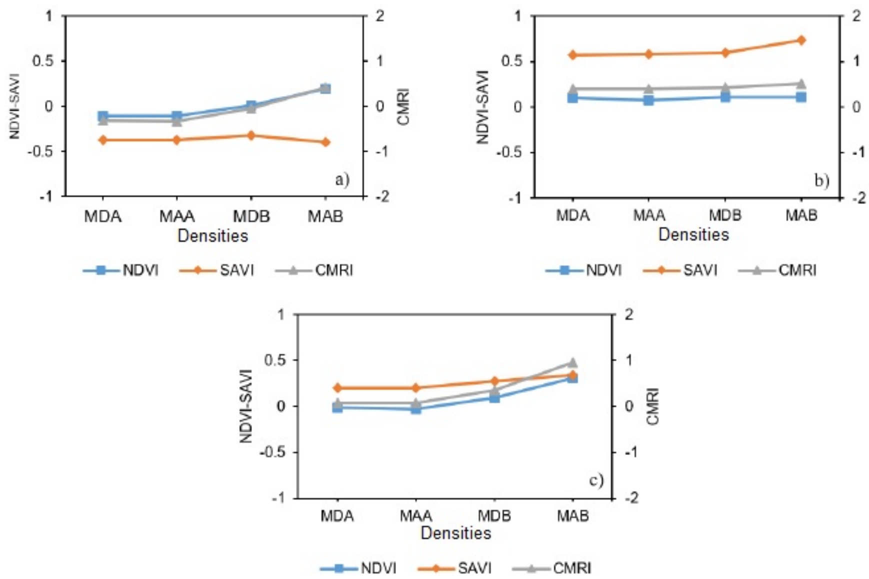

Figure 5. Behavior of vegetation indices for different mangrove densities a) 1998-2014, b) 2014-2017 and c) 1998-2017.

the increase in tides (Winarso and Purwanto, 2017; Gupta et al., 2018); on the contrary, reflectivity in the infrared band reported for 2017 showed high values (greater than 40 %) for three of the MF densities (MDA, MAA and MDB), while MAB obtained average values above 28 % in low tide conditions, results that agree with those reported by Zhang et al. (2017) and Xia et al. (2018).

The spectral sign of MF may vary due to the effects of the tide; therefore, it is affected due to the amount of water under MF at the moment of obtaining the image. Because of the latter, different spectral responses can be obtained for MF at different dates and densities. It usually tends to underestimate the mangrove surface with images that only consider a single tidal state. The latter aspect is very important for remote sensing research in mangroves Zhang and Tian (2013). The behavior of the IV values of the years 2014 and 2017 was similar to that described for infrared reflectance, but with a decrease in the value of the image in high tide, also, the value of the IVs decreased as the density of MF decreased (NDVI and CMRI better showed this situation).

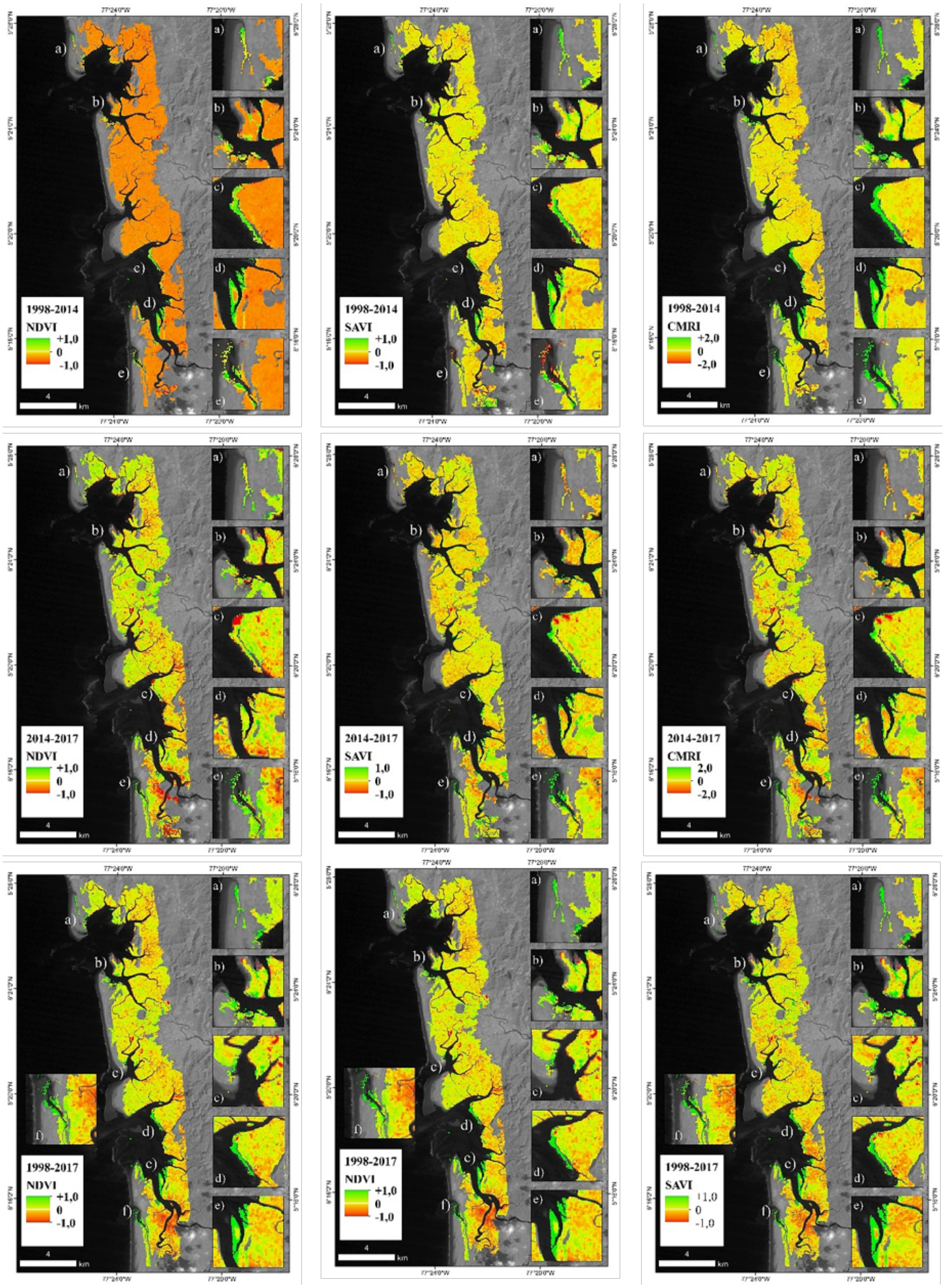

Figure 6. Vegetation indices for monitoring mangrove forests. (a), (b), (c), (d), (e), (f).

The spatial-temporal evaluation of IVs (1998-2014, 2014-2017 and 1998-2017) showed that changes in these indices occurred in the period 1998-2014, where there was an increase in the mean MAB value of 19 % in NDVI. For the period 1998-2017, the positive variation in the mean value was 31 % for NDVI, however, these variations in the IV were recorded in respect of MF located mainly in the land-sea strip, where there is a strong interaction of tide, and mangroves may be submerged periodically, generating a difference between the IV values (Jia et al., 2019; Xia et al., 2020). Similarly, when the 2014-2017 comparison was made, the mean values of NDVI and CMRI remained with a constant positive trend close to zero (0), this being the comparison of images in high tide and low tide.

The lowest SAVI value was +0.13 for MAB in the 1998 image, values that are similar to those reported by Rhyma et al. (2020) for mangroves in Malaysia using SPOT images; however, in the 1998-2014 comparison, it was observed that the average values tended to negative changes (reductions that may exceed 30 %), whereas for 2014-2017 the mean values of SAVI were greater than 50 % for all densities. This variation may be related to the findings of Rhyma et al. (2020) who noted that different values for the adjustment L factor of SAVI index should be tested at the different mangrove densities, as their value should be adjusted according to the soil moisture conditions due to the tide at each site. Similarly, Xia et al. (2020) indicated that NDVI and SAVI yield better in mangroves when analyses are performed with images captured at low tide, as IV cannot efficiently detect submerged mangroves, making characterization and monitoring difficult.

CMRI proposal is recent, but has been applied in different mangrove monitoring studies worldwide (Ahmad et al., 2019; Chen, 2020; Diniz et al., 2019; Ghosh et al., 2020). This study showed a first application of CMRI for mangrove monitoring in Colombia. The results shown indicated that MF were in constant photosynthetic production over 19 years and that the indices value demonstrated that MF in that particular site was in very good physiological condition. This IV could yield better results for images with different tidal conditions by eliminating the effect of moisture content on soil by using NDWI (Baloloy et al., 2020).

5 Conclusions

Landsat images are an important resource for mangrove monitoring, as they allow their identification through the spectral response of MF and the possibility of space-time analysis over a long period of time. Visual identification of MF in Landsat products should be done using combinations of bands, using NIR such as infrared color (NIR, Red, Green) and composite false color 1 (NIR, SWIR, Red). In this sense, the spectral response of MF is affected by the humidity conditions caused by the fluctuation of tidal conditions. The use of IVs allowed to recognize that the coastal area showed constant changes in its values. Mainly influenced by the tidal state; this aspect needs to be taken into account when analyzing IVs in MF as it is essential for the implementation of other more detailed analysis and classification processes, in order to obtain the least uncertainty possible. This study used CMRI, which is an IV developed specifically for MF studies, and in this case, it showed good yields. This research is a reference for future research in the spectral characterization and monitoring of MF with Landsat images on the northern coast of the Colombian Pacific.

Acknowledgments

This study was developed in the context of the project called: "Planning and Management of Colombian Coastal and Marine Areas" of the General Marine Office-DIMAR in Colombia. The author thanks the Center for Oceanographic and Hydrographic Research of the Pacific-CCCP and the GIS and Remote Sensing Laboratory in Tumaco for their collaboration.

References

Ahmad, Z., Luqman, M., Suharni, M., Noor, S., Taib, A., and Shaheed, M. (2019). Impact of coastal development on mangrove distribution in c6ytherating estuary, pahang, malaysia. *Malaysian Journal of Fundamental and Applied Sciences*, 15(3):456–461. Online:https://bit.ly/36OYYje.

Ariza, A. (2013). Descripción y corrección de productos landsat 8 ldcm (landsat data continuity mission) versión 1.0. Technical report, Centro de

Investigación y Desarrollo – CIAF, Instituto Geográfico Agustín Codazzi, Bogotá.

Asner, G. (1998). Biophysical and biochemical sources of variability in canopy reflectance. *Remote sensing of Environment*, 64(3):234–253. Online:https://bit.ly/3hVvgzg.

Ávila, D., Curbelo, E., Madrigal, L., and Pérez, R. (2020). Variación espacio-temporal de la respuesta espectral en manglares de la habana, cuba, evaluada con sensores remotos. *Revista de Biología Tropical*, 68(1):321–335. Online:https://bit.ly/3kF9SQM.

Baloloy, A., Blanco, A., Raymund, A., and Nadaoka, K. (2020). Development and application of a new mangrove vegetation index (mvi) for rapid and accurate mangrove mapping. *ISPRS Journal of Photogrammetry and Remote Sensing*, 166:95–117. Online:https://bit.ly/2Tw2dcq.

Bannari, A., Morin, D., Bonn, F., and Huete, A. (1995). A review of vegetation indices. *Remote sensing reviews*, 13(1-2):95–120. Online:https://bit.ly/3Bw8ENw.

Blanco, J. F., Escobar-Sierra, C., and Carvajal-Quintero, J. D. (2014). Gorgona, baudó y darién (chocó biogeográfico, colombia): ecorregiones modelo para los estudios ecológicos de comunidades de quebradas costeras. *Revista de Biología Tropical*, 62(1):43–64. Online:https://bit.ly/2UQYl6z.

Chander, G. and Markham, B. (2003). Revised landsat-5 tm radiometric calibration procedures and postcalibration dynamic ranges. *IEEE Transactions on geoscience and remote sensing*, 41(11):2674–2677. Online:https://n9.cl/wygmu.

Chen, N. (2020). Mapping mangrove in dongzhaigang, china using sentinel-2 imagery. *Journal of Applied Remote Sensing*, 14(1):1–11. Online:https://bit.ly/3hY0I06.

Chow, J. (2017). Mangrove management for climate change adaptation and sustainable development in coastal zones. *Journal of Sustainable Forestry*, 37(2):139–156. Online:https://bit.ly/36UsrbI.

Chuvieco, E. (1995). *Fundamentos de teledetección espacial*. Ediciones RIALP S.A., Madrid, 2nd ed. edition.

Chuvieco, E. (2010). *Teledetección Ambiental*. Ariel Editorial, Barcelona, 3rd ed edition.

Congalton, R. (1991). A review of assessing the accuracy of classifications of remotely sensed data. *Remote Sensing of Environment*, 37(1):35–46. Online:https://bit.ly/3kUfMgX.

Conti, L., Sampaio, C., and Cunha, M. (2016). Spatial database modeling for mangrove forests mapping; example of two estuarine systems in brazil. *Modeling Earth Systems and Environment*, 2(73):1–12. Online:https://bit.ly/3kPkInf.

DIMAR-CCCP (2013). Zonificación fisiográfica del litoral pacífico colombiano. fase i. Technical report, Dirección General Marítima-Centro de Investigaciones Oceanográficas e Hidrográficas del Pacífico, Dirección General Marítima: San Andrés de Tumaco.

Diniz, C., Cortinhas, L., Nerino, G., Rodrigues, J., Sadeck, L., Adami, M., and Souza, P. (2019). Brazilian mangrove status: Three decades of satellite data analysis. *Remote Sensing*, 11(7):1–19. Online:https://bit.ly/3y78oCI.

Dirección General Marítima., editor (2020). *Red de Medición de Parámetros Oceanográficos y de Meteorología Marina (REDMPOMM). Infraestructura de Datos Espaciales Marítima, Fluvial y Costera de Colombia*.

ESRI (2014). *ArcGIS Desktop 10.3., Environmental Systems Research Institute*. Redlands, USA.

FAO (2007). *The world's mangroves 1980-2005*. Food and Agriculture Organization of the United Nations.

Franco, R. (2017). *Composiciones Landsat en ARCGIS. Guía Básica*, MIXDYR. Online: https://bit.ly/3iXYcWX edition.

Galeano, A., Urrego, L., Botero, V., and Bernal, G. (2017). Mangrove resilience to climate extreme events in a colombian caribbean island. *Wetlands ecology and management*, 25(6):743–760. Online:https://bit.ly/36UD5PJ.

Gao, B. (1996). Ndwi a normalized difference water index for remote sensing of vegetation liquid water from space. *Remote Sensing of Environment*, (358):257–266. Online:https://bit.ly/3x1kps2.

Ghosh, S., Bakshi, M., Gupta, K., Mahanty, S., Bhattacharyya, S., and Chaudhuri, P. (2020). A preliminary study on upstream migration of mangroves in response to changing environment along river hooghly, india. *Marine pollution bulletin*, 151:1–14. Online:https://bit.ly/3iFWKYT.

Giri, C. (2016). Observation and monitoring of mangrove forests using remote sensing: Opportunities and challenges. *Marine pollution bulletin*, 8(9):1–8. Online:https://bit.ly/3iCgAV0.

Gupta, K., Mukhopadhyay, A., Giri, S., Chanda, A., Majumdar, S., Samanta, S., Mitra, D., Samal, R., Pattnaik, A., and Hazra, S. (2018). An index for discrimination of mangroves from non-mangroves using landsat 8 oli imagery. *MethodsX*, 5:1129–1139. Online:https://bit.ly/2UzJIEz.

Holdridge, L. (1978). *Ecología basada en zonas de vida*. Centro Interamericano de Documentación e Información Agrícola-IICA.

Horning, N. (2014). Selecting the appropriate band combination for an rgb image using landsat imagery version 1.0.

Huete, A. (1988). A soil-adjusted vegetation index (savi). *Remote sensing of environment*, 25(3):295–309. Online:https://bit.ly/3zuX8jY.

Jia, M., Wang, Z., Wang, C., Mao, D., and Zhang, Y. (2019). New vegetation index to detect periodically submerged mangrove forest using single-tide sentinel-2 imagery. *Remote Sensing*, 11:1–17.Online: https://bit.ly/3iToERo.

Kuenzer, C., Bluemel, A., Gebhardt, S., Quoc, T., and Dech, S. (2011). Remote sensing of mangrove ecosystems: A review. *Remote Sensing*, 3(5):878–928. Online:https://bit.ly/2UHovII.

Mohamed, E. (2017). Consideration of landsat-8 spectral band combination in typical mediterranean forest classification in halkidiki, greece. *Open Geosciences*, 9(1):468–479. Online:https://bit.ly/36Zo7Yt.

Mondal, P., Trzaska, S., and De Sherbinin, A. (2018). Landsat-derived estimates of mangrove extents in the sierra leone coastal landscape complex during 1990–2016. *Sensors*, 18(12):1–15. Online:https://bit.ly/3BxOpiF.

Monirul, I., Helena, B., and Lalit, K. (2018). Monitoring mangrove forest land cover changes in the coastline of bangladesh from 1976 to 2015. *Geocarto International*, 31(13):1458–1476. Online:https://bit.ly/2VbEcI1.

Muhsoni, F., Sambah, A., Mahmudi, M., and Wiadnya, D. (2018). Comparison of different vegetation indices for assessing mangrove density using sentinel-2 imagery. *Int. J. Geomate*, 14:42–51. Online:https://bit.ly/3eMwOcT.

Omar, H., Misman, M., and Linggok, V. (2018). Characterizing and monitoring of mangroves in malaysia using landsat-based spatial-spectral variability. In *IOP Conference Series: Earth and Environmental Science*, volume 169, pages 24–25. Online:https://bit.ly/3hWSAwK.

Pagkalinawan, E. (2014). Mangrove forest mapping using landsat 8 images. *State of the mangrove summit: Northwestern Luzon Proceedings*, pages 60–64. Online:https://bit.ly/2TxBOLj.

Perea-Ardila, M., Oviedo-Barrero, F., and Leal-Villamil, J. (2019). Cartografía de bosques de manglar mediante imágenes de sensores remotos: estudio de caso: Buenaventura, colombia. *Revista de Teledetección*, 53(1):73–86. Online:https://bit.ly/3ygOWU8.

Pérez, F. and De la Riva, J. (1998). El empleo de imágenes landsat tm para la detección y cartografía de áreas incendiadas en el prepirineo occidental oscense. *Geographicalia*, (36):131–145. Online:https://bit.ly/36XtEij.

Pham, T., Yokoya, N., Bui, D., Yoshino, K., and Friess, D. (2019). Remote sensing approaches for monitoring mangrove species, structure, and biomass: Opportunities and challenges. *Remote Sensing*, 11(3):1–24. Online:https://bit.ly/3rFlMf2.

Pimple, U., Simonetti, D., Sitthi, A., Pungkul, S., Leadprathom, K., Skupek, H., Som, J., Gond, V., and Towprayoon, S. (2018). Google earth engine based three decadal landsat imagery analysis for mapping of mangrove forests and its surroundings in the trat province of thailand. *Journal of Computer and Communications*, 6:246–264. Online:https://bit.ly/3BBa7SU.

Purwanto, A. and Asriningrum, W. (2019). Identification of mangrove forests using multispectral satellite imageries. *International Journal of Remote Sensing and Earth Sciences (IJReSES)*, 16(1):63–86. Online:https://bit.ly/36YbtJn.

Rebelo-Mochel, F. and Ponzoni, F. (2007). Spectral characterization of mangrove leaves in the brazilian amazonian coast: Turiaçu bay, maranhão state. *Anais da Academia Brasileira de Ciências*, 79(4):683–692. Online:https://bit.ly/3rEKZGj.

Rhyma, P., Norizah, K., Hamdan, O., Faridah, I., and Zulfa, A. (2020). Integration of normalised different vegetation index and soil-adjusted vegetation index for mangrove vegetation delineation. *Remote Sensing Applications: Society and Environment*, 17:1–70. Online:https://bit.ly/3y2s4ru.

Rodríguez-Rodríguez, J., Sierra-Correa, P., Gómez-Cubillos, M., and Villanueva, L. (2016). *The Wetland Book*, chapter Mangroves of Colombia. Springer Netherlands, Dordrecht.

Rouse, J., Haas, R. Shell, J., and Deering, D. (1974). *Monitoring vegetation systems in the Great Plains with ERTS*. Goddard Space Flight Center.

Umroh, A. and Sari, S. (2016). Detection of mangrove distribution in pongok island. *Procedia Environmental Sciences*, 33:253–257. Online:https://n9.cl/w48d.

USGS (1998). Usgs eros archive - landsat archives - landsat 4-5 thematic mapper (tm) level-1 data products. In *Landsat 4-5 TM Collection 1*, Landsat Scene ID LT50100561998003CPE00. U.S Geological Survey. Online:https://bit.ly/3b7KDjI.

USGS (2014). Usgs eros archive - landsat archives - landsat 8 oli level-1 data products. In *Landsat 8 Operational Land Imager (OLI) Collection 1*, Landsat Scene ID LC80100562014239LGN01. U.S Geological Survey. Online:https://bit.ly/3b7KDjI.

USGS (2017). Usgs eros archive - landsat archives - landsat 7 etm+ level-1 data products. In *Landsat 7 Enhanced Thematic Mapper Plus (ETM+) Collection 1*, Landsat Scene ID LE70100562017111EDC00. U.S Geological Survey. Online:https://bit.ly/3b7KDjI.

USGS (2018a). Landsat 7 data users handbook. version 2.0. Technical report, U.S Geological Survey.

USGS (2018b). Landsat 8 data users handbook - versión 3.0. Technical report, U.S Geological Survey.

USGS (2020). Earthexplorer. software, U.S Geological Survey.

Vaghela, B., Parmar, M., Solanki, H., Kansara, B., Prajapati, S., and Kalubarme, M. (2018). Multi criteria decision making (mcdm) approach for mangrove health assessment using geo-informatics technology. *International Journal of Environment and Geoinformatics*, 5(2):114–131. Online:https://bit.ly/3rx4Zuo.

Wang, L., Jia, M., Yin, D., and Tian, J. (2019). A review of remote sensing for mangrove forests: 1956-2018. *Remote Sensing of Environment*, 231:1–150. Online:https://bit.ly/2WcAxdr.

Wilkie, M. and Fortuna, S. (2003). *Status and trends in mangrove area extent worldwide*. Food and Agriculture Organization of the United Nations.

Winarso, G. and Purwanto, A. (2017). Evaluation of mangrove damage level based on landsat 8 image. *International Journal of Remote Sensing and Earth Sciences*, 11(2):105–116. Online:https://bit.ly/3rutwjS.

Xia, Q., Qin, C., Li, H., Huang, C., and Su, F. (2018). Mapping mangrove forests based on multi-tidal high-resolution satellite imagery. *Remote Sensing*, 10(1343):2–20. Online:https://bit.ly/3l6iPD5.

Xia, Q., Qin, C., Li, H., Huang, C., Su, F., and Jia, M. (2020). Evaluation of submerged mangrove recognition index using multi-tidal remote sensing data. *Ecological Indicators*, 113:1–140. Online:https://bit.ly/3kRKpDH.

Zhang, X. and Tian, Q. (2013). A mangrove recognition index for remote sensing of mangrove forest from space. *Current Science*, 105(8):1149–1155. Online:https://bit.ly/3i0V11a.

Zhang, X., Treitz, P., Chen, D., Quan, C., Shi, L., and Li, X. (2017). Mapping mangrove forests using multi-tidal remotely-sensed data and a decision-tree-based procedure. *International journal of applied earth observation and geoinformation*, 62:201–214. Online:https://bit.ly/3i0jVOr.

Zhu, Z. and Woodcock, C. (2014). Automated cloud, cloud shadow, and snow detection in multitemporal landsat data: An algorithm designed specifically for monitoring land cover change. *Remote Sensing of Environment*, 152:217–234. Online:https://bit.ly/3ByuHDD.